2023 IEEE/ASME International Conference on Advanced Intelligent Mechatronics (AIM)
June 28-30, 2023. Seattle, Washington, USA

A New Torque Estimation Method Based on Equivalent Efficiency Model and BP Neural Network of Mechatronic Integrated Joint

Junjie Dai[1,2], Xin Yang[3], Chin-Yin Chen[1,*], Guilin Yang[1] and Han Chen[1,4]

***Abstract*— This paper proposed a new torque estimation method based on an equivalent efficiency model and back propagation (BP) neural network to obtain accurate torque. Firstly, the joint transmission efficiency model is obtained based on experiments to correct the torque observer (TOB). Then the relationship between joint position, velocity, current, and torque estimation is established by BP neural network, and the torque estimation error is compensated further. Finally, several comparative experiments are carried out. The results show that the proposed method can obtain more accurate torque compared with traditional TOB.**

I. INTRODUCTION

With the rapid development of manufacturing and service industries, people have higher human-robot interaction (HRI) performance requirements. The robots not only should ensure humans' safety but also can cooperate with them to complete complex work. Therefore, accurately measuring and controlling the external force or torque from the environment or humans have become the key to realizing HRI. But so far, many technical problems still need to be overcome in the research on collaborative robots. Due to the reduction mechanism (harmonic reducer) in the integrated joint, on the one hand, its flexibility is introduced into the joint system, which increases the difficulty of modeling. On the other hand, there is a difference in the harmonic reducer's forward and back transmission efficiency models. Both of them will influence the performance of HRI. In addition, torque sensors are often installed in the integrated joints to realize related torque control algorithms. However, the introduction of torque sensors not only increases the cost of the integrated joint but also further reduces the stiffness of the joint system, making the design of the integrated joint controller more difficult.

To solve the difficulty mentioned above, many scholars have been studying the torque observer (TOB) structure that does not rely on sensors in recent years. The traditional method used the current and velocity signal to estimate the torque value based on the dynamic model[1]. Combining it with the disturbance observer (DOB), the system could realize the sensorless force/torque control[2][3]. However, this method had high requirements for the dynamic model, especially the friction model, which was complex and nonlinear. Based on the generalized momentum method, Wahrburg estimated the environmental force and joint torque to detect whether the robot collides[4]. But this method was also highly dependent on the model. Peng obtained the model of joint torque through an offline/online neural network[5]. Kommuri designed a higher-order sliding-mode-based observer to estimate the external torque online against nonlinear friction[6]. Some scholars applied Extended Kalman Filter (EKF) to estimate the external joint torques[7][8]. These methods are independent of the model, but there is still room for further improvement in the estimation accuracy.

In this paper, the equivalent efficiency model is established and corrected based on the traditional TOB, which significantly reduces the estimation error of TOB. In addition, to improve the estimation accuracy further, the back propagation (BP) neural network structure is designed using the integrated joint's state information.

The rest of this paper is organized as follows. The equivalent efficiency model of the integrated joint is established and analyzed in Section II. In Section III, BP neural network is introduced to improve the torque estimation accuracy further. Section IV performs several experiments and analyzes the results. Finally, the conclusion is summarised in Section V.

II. EQUIVALENT EFFICIENCY MODEL OF THE INTEGRATED JOINT

The internal mechanical structure of the integrated joint can be simplified as a transmission diagram, as shown in Fig.1. It contains motor-side, reduction gear, and load-side. Among them, the reduction gear is usually a harmonic reducer. τ_m, τ_j, and τ_l^{ext} represent the motor torque, the joint torque of the flexible spline of the harmonic reducer, and the torque applied to the joint by the environment or humans, respectively. The motor-side inertia and damping are represented by J_m and D_m. And the load-side inertia and damping are defined as J_l and D_l. For reduction gear, K, D, G_r, and η denote its stiffness, damping, gear ratio, and efficiency. θ_m and θ_l are the positions of the motor-side and load-side. In Fig.1, the forward drive means normal joint control that operates according to a command signal. In

*This work was supported by the Key R&D Program of Zhejiang Province (2022C01101, 2021C01067, 2021C01070), the National Natural Science Foundation of China (U20A20282, 92048201, U21A20121), the Ningbo Science and Technology Innovation 2025 Major Special Project (2021Z128, 2021Z068).

[1]Junjie Dai, Chin-Yin Chen, Guilin Yang and Han Chen are with Zhejiang Key Laboratory of Robotics and Intelligent Manufacturing Equipment Technology, Ningbo Institute of Materials Technology and Engineering, Ningbo 315201, China. daijunjie, chenchinyin, glyang, chenhan@nimte.ac.cn

[2]Junjie Dai is also with University of Chinese Academy of Sciences, Beijing 100049, China.

[3]Xin Yang is with Zhejiang Zeekr Intelligent Technology Co., Ltd., Ningbo 315800, China. yangxin19@mails.ucas.ac.cn

[4]Han Chen is also with College of Mechanical Engineering, Zhejiang University of Technology, Hangzhou, 310023, China

[*]Chin-Yin Chen is the corresponding author.

contrast, the back drive means the joint control that operates according to an external torque.

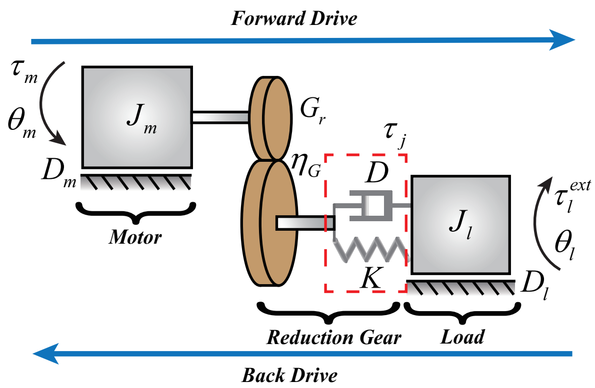

Fig. 1. The transmission system of integrated joint

The integrated joint can be regarded as a dual mass-damping-spring system based on its internal structure. Its dynamic equations can be obtained:

$$\tau_m - \frac{\tau_j}{G_r}\eta_G = J_m\ddot{\theta}_m + D_m\dot{\theta}_m \tag{1}$$

$$\tau_j - \tau_l^{ext} = J_l\ddot{\theta}_l + D_l\dot{\theta}_l \tag{2}$$

$$\tau_j = K\left(\frac{\theta_m}{G_r} - \theta_l\right) + D\left(\frac{\dot{\theta}_m}{G_r} - \dot{\theta}_l\right) \tag{3}$$

In (3), the joint torque is calculated according to the positions and velocities of the motor-side and the load-side. However, due to the nonlinear joint stiffness and the lag of the velocities and positions, the torque error estimated by this method is relatively large. Fig. 2 shows the block diagram of TOB in the integrated joint.

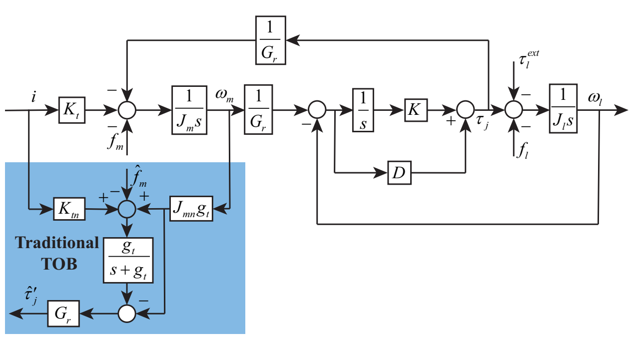

Fig. 2. Block diagram of TOB in integrated joint

In Fig.2, i and K_t denote motor input current and torque constant. ω_m and ω_l represent the velocities of motor-side and load-side, respectively. $\hat{\tau}_j{}'$ is the estimation of the joint torque by traditional TOB. f_m is the friction torque, which contains motor-side viscosity and nonlinear friction. And $\hat{f}_m$ denote the friction torque estimation of the motor-side. g_t is the bandwidth of TOB. Therefore, the joint torque τ_j is estimated using current i and motor-side velocity ω_m as follows:

$$\hat{\tau}_j{}' = \left[\frac{g_t}{s+g_t}\left(iK_{tn} + J_{mn}g_t\omega_m - \hat{f}_m\right) - J_{mn}g_t\omega_m\right]G_r \tag{4}$$

However, this estimation method neglects the reducer stiffness, transmission efficiency, and other nonlinear factors. Especially when the joint state or external load changes, the traditional TOB has a large estimation error. On the other hand, most friction models cannot accurately describe the friction in the joint, especially in the low-velocity stage. Besides, since the direction of the static friction force is difficult to determine, the calculation of the friction model often has a large error with the actual friction, which further reduces the accuracy of TOB.

Due to the existence of the harmonic reducer, the integrated joint inevitably has forward and back drive efficiency. It is due to the friction generated during the transmission process that consumes part of the energy. In general, transmission efficiency is related to the load, velocity, and temperature, among which the load significantly influences the efficiency. In addition, the unique transmission form of the harmonic reducer and its flexibility lead to different torque forms of the circular spline and the flexible spline during forward and back drive. That makes an apparent difference between the forward and back drive efficiency models. Therefore, it is challenging to establish an efficiency model based on the physical model of the integrated joint. In this section, the model under different velocities and loads is attained by fitting the experimental data.

Since friction is the main cause of transmission efficiency, the damping in the original system can be neglected. According to its main influence on joint dynamics rather than kinematics, it can be simplified as a correction coefficient η of reaction force. So the block diagram of TOB based on an equivalent efficiency model is shown in Fig. 3.

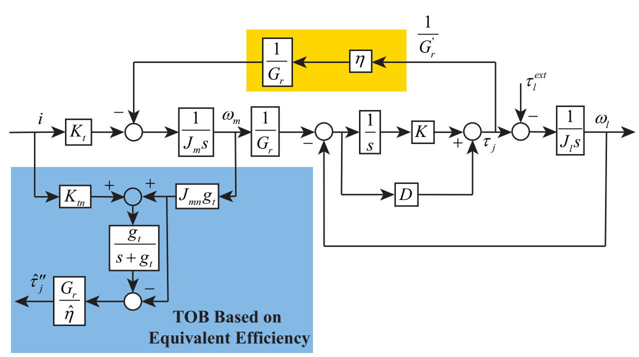

Fig. 3. Block diagram of TOB based on equivalent efficiency in integrated joint

The relationship of motor-side can be expressed as:

$$iK_t - \frac{\eta\tau_j}{G_r} = J_m\dot{\omega}_m \tag{5}$$

when the joints move with a constant velocity, (5) can be simplified as:

$$\eta = \frac{G_r iK_t}{\tau_j} \tag{6}$$

Therefore, η can be calculated by measuring the motor's current and the load torque when the joint moves with a constant velocity. According to the research of other scholars, load and velocity are the main factors affecting efficiency. Since the purpose of this research is to estimate the joint torque, the load of the joint is indirectly characterized by the output torque of the motor. The velocity can be directly obtained by the encoder signal. Therefore, the correction coefficient η is subsequently fitted by the joint velocity, the load torque, and the input motor current in this section. Finally, combining with the traditional TOB method, the estimation of joint torque $\hat{\tau}_j{''}$ can be written as:

$$\hat{\tau}_j{''} = \left[\frac{g_t}{s+g_t} \left(iK_{tn} + J_{mn} g_t \omega_m \right) - J_{mn} g_t \omega_m \right] G_r / \hat{\eta} \qquad (7)$$

To better fit the influence of transmission efficiency on joint dynamic performance. Experiments are designed for two cases of forward and back drive efficiencies. When simulating the forward drive, a velocity loop control is performed on the tested joint, and a current loop control is performed on the driving joint. In this case, the current direction of the tested joint is the same as the velocity direction. So the current drives the joint movement, and the load hinders the joint movement. The desired velocities of the tested joints are set to 0.2rad/s, 0.6rad/s, 1.0rad/s, 1.4rad/s, 1.8rad/s, 2.2rad/s, 2.6rad/s, and 3.0rad/s, respectively. Due to the limitation of the nominal output torque, when the joint velocity is less than ±1.8rad/s, the input current corresponding to the driving joint at each velocity is 0A, 1A, 2A, 3A, 4A, and 5A. When the velocity exceeds ±1.8rad/s, the input current of the driving joint at each velocity is 0A, 1A, 2A, 3A, and 4A, respectively. The motor-side velocity and input current of the tested joint, the input current of the driving joint, and the load torque are shown in Fig. 4.

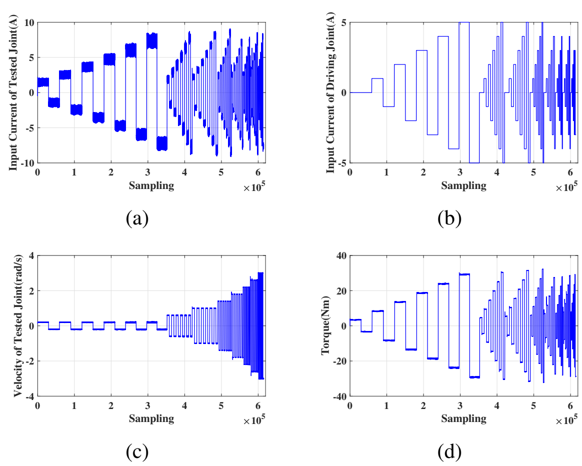

Fig. 4. Forward drive: (a) Input current of tested joint; (b) Input current of driving joint; (c) Motor-side velocity of tested joint; (d) Joint torque.

When simulating the back drive, the current loop control is performed on the tested joint, and the velocity loop control is performed on the driving joint. In this case, the current direction of the joint to be tested is opposite to the velocity direction, the load drives the joint movement, and the current hinders the joint movement. Similarly, the desired velocities of the driving joint, and the current of the tested joint at each velocity are set as the same as those in forward drive. The motor-side velocity and input current of the tested joint, the input current of the driving joint, and the load torque are shown in Fig. 5.

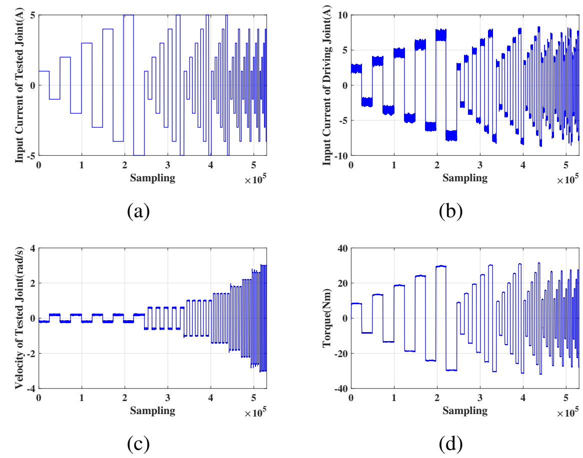

Fig. 5. Back drive: (a) Input current of tested joint; (b) Input current of driving joint; (c) Motor-side velocity of tested joint; (d) Joint torque.

It can be found that the joint velocity and the input current are stable in both the forward and back drive. But there are large overshoots at high velocities when changing directions. The joint torque has a slight vibration due to the harmonic reducer torque ripple. Then the torque and the current measured at the same velocity and load are averaged. And the correction coefficient η in the corresponding state can be obtained according to (6).

Then η can be fitted as a binary function of motor-side velocity and input current. However, there is a difference between the forward and back drive models. On the other hand, the friction model parameters are also different when the integrated joint is in positive and negative rotation. Therefore, the results are divided into four cases to fit ($i>0$, $\omega_m>0$; $i<0$, $\omega_m<0$; $i<0$, $\omega_m>0$; $i>0$, $\omega_m<0$). Here, $\omega_m>0$ represents positive rotation, and $\omega_m<0$ represents negative rotation. The same symbol of i and ω_m represents the forward drive, and the opposite symbol of i and ω_m represents the back drive. Due to the unknown physical model of efficiency, the polynomial fitting based on the least square method is adopted. Through comparative analysis, the root mean square error (RMSE) can be controlled below 0.06 by a quadratic polynomial. Although higher-order models can match the test data better, they are prone to overfitting. The fitting function of $\hat{\eta}$ is shown in (8):

$$\hat{\eta} = p_{00} + p_{10} i + p_{01} \omega_m + p_{20} i^2 + p_{11} i \omega_m + p_{02} \omega_m^2 \qquad (8)$$

The experimental data and model fitting results of four cases are shown in Fig. 6 and Tab. I.

III. TORQUE ESTIMATION METHOD BASED ON THE BP NEURAL NETWORK

However, even if as much experimental data is collected as possible, it is still impossible to cover all operating

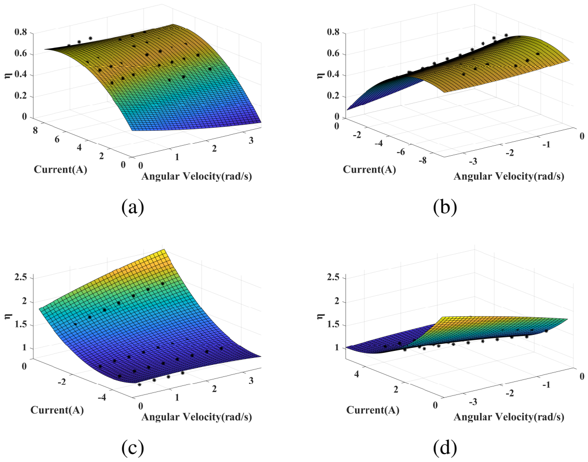

Fig. 6. The measurement data of η and model fitted results: (a) $i > 0$, $\omega_m > 0$; (b) $i < 0$, $\omega_m < 0$; (c) $i < 0$, $\omega_m > 0$; (d) $i > 0$, $\omega_m < 0$.

TABLE I
MODEL PARAMETERS AND RMSE OF η

Cases	$i > 0$, $\omega_m > 0$	$i < 0$, $\omega_m < 0$	$i < 0$, $\omega_m > 0$	$i > 0$, $\omega_m < 0$
P_{00}	0.2530	0.2850	1.8830	1.8660
P_{10}	0.1493	-0.1430	0.4870	-0.4769
P_{01}	-0.0820	0.0839	0.2602	-0.2342
P_{20}	-0.0117	-0.0114	0.0658	0.0645
P_{11}	0.0060	0.0059	0.0435	0.04295
P_{02}	0.0066	0.0060	-0.0168	-0.0101
RMSE	0.01963	0.01719	0.05599	0.05504

conditions. So the torque estimation method based on the equivalent efficiency model still has some errors. In this section, BP neural network method is introduced, which can fit the characteristics of any nonlinear system. Therefore, it can improve the accuracy of torque estimation further. Since θ_m, ω_m, θ_l, ω_l, $\hat{\tau}_j''$ are related to joint output torque directly. Besides, i can characterize the load information, which is conducive to obtaining a more accurate torque model. So set to the input of the neural network $x = \left[i, \theta_m, \omega_m, \theta_l, \omega_l, \hat{\tau}_j''\right]$, and the desired output τ_j is the value of the torque sensor. Since the number of input variables is small, and the multiple hidden layers can be used to fit nonlinear functions, the number of hidden layers is set to 3. The number of neurons is 20, 40, and 10, respectively. The activation function is selected as tanh:

$$\sigma(x) = \frac{1 - e^{-x}}{1 + e^{-x}} \tag{9}$$

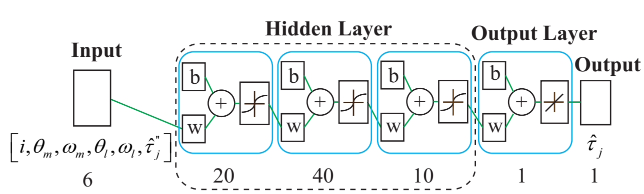

Fig. 7. Neural network for torque estimation of joint.

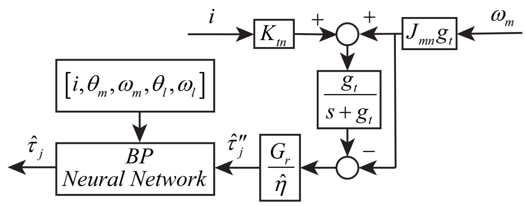

Fig. 8. TOB based on the equivalent efficiency model and BP neural network.

The whole neural network structure is shown in Fig. 7, and the TOB based on the equivalent efficiency model and BP neural network is shown in Fig. 8. To obtain sufficient dynamic information on the joint at different velocities and accelerations, using periodic Fourier Series as excitation trajectory of the joint. Integrated joint's motor-side position, velocity, and acceleration as shown in (10):

$$\begin{cases} \theta_m(t) = \sum_{i=1}^{N} \left[\frac{a_i}{i\omega} \sin(i\omega t) - \frac{b_i}{i\omega} \cos(i\omega t) \right] + \sum_{j=1}^{6} c_j t^{j-1} \\ \omega_m(t) = \sum_{i=1}^{N} \left[a_i \cos(i\omega t) + b_i \sin(i\omega t) \right] + \sum_{j=2}^{6} c_j (j-1) t^{j-2} \\ \dot{\omega}_m(t) = \sum_{i=1}^{N} \left[-i\omega a_i \sin(i\omega t) + i\omega b_i \cos(i\omega t) \right] \\ \qquad + \sum_{j=3}^{6} c_j (j-1)(j-2) t^{j-3} \end{cases} \tag{10}$$

The trajectory is the sum of N sine and cosine functions, where ω is the fundamental frequency of the Fourier Series. a_i and b_i are the amplitudes of sine and cosine function, respectively. $\sum_{j=1}^{6} c_j t^{j-1}$, $\sum_{j=2}^{6} c_j (j-1) t^{j-2}$ and $\sum_{j=3}^{6} c_j (j-1)(j-2) t^{j-3}$ denote the joint position, velocity and acceleration compensation, which can be calculated according to the actual required initial and final states. By designing and combining multiple trajectories, the trajectories are transitioned by a curve with a velocity of zero for 2s. This enables the neural network to better fit the dynamic model of the integrated joint at start and stop. The position, velocity, and acceleration are shown in Fig. 9.

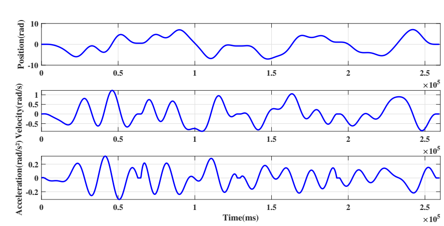

Fig. 9. Position, velocity, and acceleration of excitation trajectory.

It can be found that the Fourier Series trajectory position and velocity obtained by genetic algorithm cover the full range of the integrated joint. So it satisfies the requirements of neural network excitation trajectory. Besides, the current trajectory generated by the same method is shown in Fig. 10.

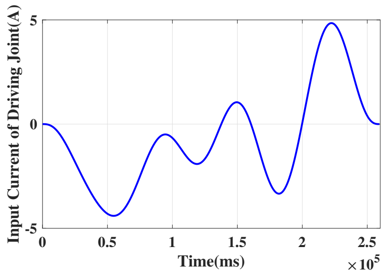

Fig. 10. Input current of the driving joint corresponds to the excitation trajectory.

When the input current of the driving motor varies, the load also changes, which can be measured in real-time by the torque sensor. The joint is controlled with a velocity loop, and the results are shown in Fig. 11.

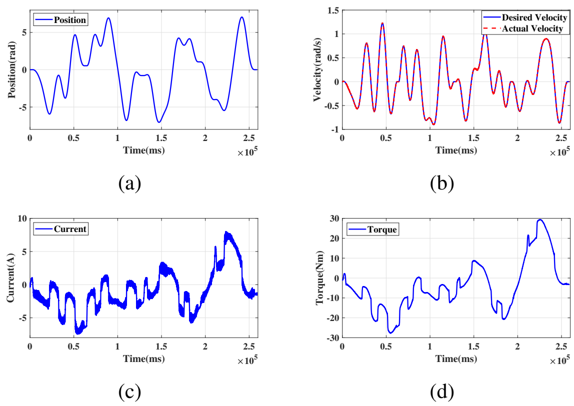

Fig. 11. Excitation trajectory velocity control: (a) Position; (b) Velocity; (c) Current; (d) Torque.

According to Fig. 11(b), the velocity control error is within 0.01rad/s, which is consistent with the planned excitation trajectory. So it is trained as sample data of neural network. The final training results are shown in Fig. 12. At the 1000th iteration, the minimum mean square error is 0.003, which satisfies the error requirements.

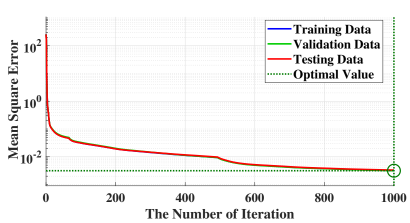

Fig. 12. Joint torque fitting results by BP neural network.

IV. EXPERIMENTS

A double-joint towing experimental platform is designed to apply a stable and controllable load to the integrated joint to carry out experiments under different loads. As shown in Fig. 13, the platform has two integrated joints and they connect with each other through a torque sensor (model: HBM T40B). The tested joint needs to measure the correction coefficient η. The driving joint is used to apply load to the tested joint. The value of the applied load is measured by the torque sensor. The joint velocity is obtained by the encoder at the motor-side of tested joint. Several comparative experiments are carried out to verify the effectiveness of the torque estimation method based on equivalent efficiency model and BP neural network.

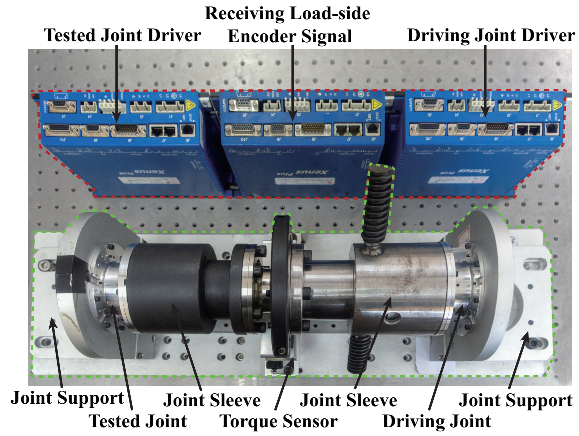

Fig. 13. Double-joint towing experimental platform.

A. Constant Velocity Control

The driving joint is used to apply a load to the tested joint. The following two cases are experimentally verified.

- *Forward Drive* The tested joint performs a velocity loop with commands of 0.5rad/s, 1.5rad/s, and 2.5rad/s, respectively. And the driving joint runs a current loop. When the velocity is ±0.5rad/s, the current commands are 0.5A, 1.5A, and 2.5A; When the velocity becomes ±1.5rad/s, the current commands are 1.5A, 2.5A, and 3.5A; Finally, the device performs with the velocity of ±2.5rad/s, the current commands are 2.5A, 3.5A, and 4.5A, respectively.
- *Back Drive* The tested joint performs a current loop, and the driving joint runs a velocity loop. Their current and velocity commands are same as those in *Forward Drive*.

The estimation results are shown in Fig. 14. In the back drive, the torque error of the traditional TOB (red dashed line) is small when the load is small. However, with the load increases, the error increases obviously. This is because that the torque loss is mainly friction at small loads. The traditional TOB has a high estimation accuracy. When the load becomes large, the joint torque is affected by efficiency mainly, so the traditional TOB estimation error increases. When the velocity is 2.5rad/s, and the load is 30Nm, the torque error is the largest (27.6%). However, whether in the forward or back drive, the torque error of TOB based on the equivalent efficiency model method (yellow dotted line) is reduced significantly compared with traditional TOB estimation. This is mainly because the established correction

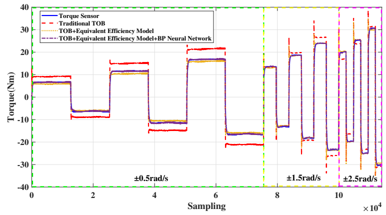

(a)

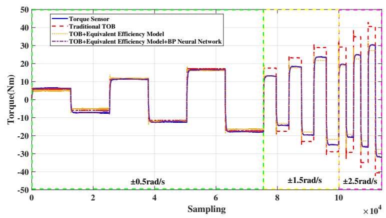

(b)

Fig. 14. Comparison of different torque estimation methods under constant velocity: (a) forward drive; (b) back drive.

model has no clear physical meaning and can not compensate all errors. It can be seen that the TOB based on equivalent efficiency model and BP neural network (purple dot-dash line) can accurately estimate the joint torque at any velocity and load.

B. Variable Velocity Control

The variable velocity control experiment is still carried out through the experimental platform of Fig. 13. A new trajectory is designed based on Fourier Series, as shown in Fig. 15.

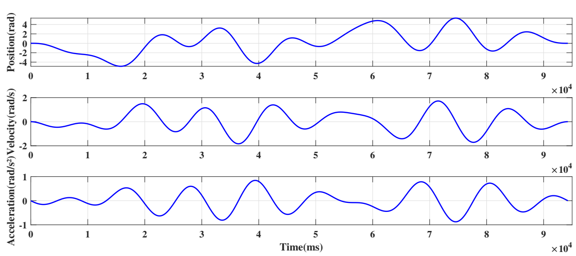

Fig. 15. Trajectory of variable velocity control experiment.

The integrated joint performs variable velocity control according to the generated trajectory. The comparison experimental results are shown in Fig. 16.

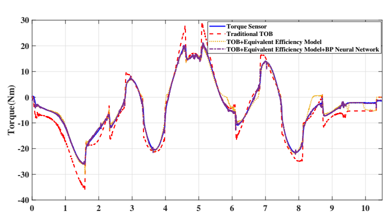

Fig. 16. Comparison of different torque estimation methods under variable velocity.

The traditional TOB has the largest error, and its mean square error (MSE) is 10.07Nm. The MSE of the TOB based on the equivalent efficiency model is 1.97Nm. However, the TOB based on the equivalent efficiency model and BP neural network has the smallest error, with a MSE of 0.22Nm. It can be seen that the accuracy of the torque estimation method proposed in this paper is much higher than that of the traditional TOB. However, when the forward and back driving switches, there are large errors in other estimation methods except for neural network estimation. This is mainly due to the difference of joint model between forward and back drive.

V. CONCLUSIONS

In this paper, the torque estimation method based on an equivalent efficiency model and BP neural network is proposed. Compared to the traditional TOB, the proposed method has higher estimation accuracy through theoretical analysis and experimental verification. Especially the joint has a large load or applies back driving. Therefore, the torque information of the joint can be obtained without a torque sensor. It not only saves the cost but also improves the dynamic performance of the joint. In the future, we will focus on the sensorless joint torque control experiment based on this estimation method.

REFERENCES

[1] T. Murakami, F. Yu, and K. Ohnishi, "Torque sensorless control in multidegree-of-freedom manipulator," *IEEE Transactions on Industrial Electronics*, vol. 40, no. 2, pp. 259–265, 1993.

[2] Y. Fukushima and K. Naemura, "Estimation of the friction force during the needle insertion using the disturbance observer and the recursive least square," *Robomech Journal*, vol. 1, no. 1, pp. 1–8, 2014.

[3] E. Sariyildiz and K. Ohnishi, "An adaptive reaction force observer design," *IEEE/ASME Transactions on Mechatronics*, vol. 20, no. 2, pp. 750–760, 2014.

[4] A. Wahrburg, E. Morara, G. Cesari, B. Matthias, and H. Ding, "Cartesian contact force estimation for robotic manipulators using kalman filters and the generalized momentum," in *2015 IEEE International Conference on Automation Science and Engineering (CASE)*. IEEE, 2015, pp. 1230–1235.

[5] G. Peng, C. Yang, W. He, Z. Li, and D. Kuang, "Neural-learning enhanced admittance control of a robot manipulator with input saturation," in *2017 Chinese Automation Congress (CAC)*. IEEE, 2017, pp. 104–109.

[6] S. K. Kommuri, S. Han, and S. Lee, "External torque estimation using higher order sliding-mode observer for robot manipulators," *IEEE/ASME Transactions on Mechatronics*, vol. 27, no. 1, pp. 513–523, 2022.

[7] L. Roveda, D. Riva, G. Bucca, and D. Piga, "External joint torques estimation for a position-controlled manipulator employing an extended kalman filter," in *2021 18th International Conference on Ubiquitous Robots (UR)*, 2021, pp. 101–107.

[8] S. Liu, L. Wang, and X. V. Wang, "Sensorless force estimation for industrial robots using disturbance observer and neural learning of friction approximation," *Robotics and Computer-Integrated Manufacturing*, vol. 71, p. 102168, 2021. [Online]. Available: https://www.sciencedirect.com/science/article/pii/S0736584521000521